Few NV Center Nanodiamonds Enable High-Speed and High-Resolution Sensing of Paramagnetic Species

Aparajita Modak, Ayan Majumder, Madhur Parashar, Siddharth Tallur, Kasturi Saha
Department of Electrical Engineering, *IIT Bombay*, Mumbai, India
214076004, 194076009, 30004898, stallur, kasturis@iitb.ac.in

***Abstract*—Nitrogen vacancy (NV) centers in diamonds are a highly promising quantum sensing platform for various applications, including biosensing of magnetically tagged biomolecules. In this work, we have studied the interaction of an ensemble of nanodiamonds (NDs), each containing few (< 5) NV centers, with paramagnetic nanoparticles, through numerical simulations and experiments. Change in the NV center properties is interrogated by performing T_1 relaxometry and optically detected magnetic resonance (ODMR) measurements.**

***Index Terms*—NV center, nanodiamond, relaxometry, magnetic nanoparticle, optically detected magnetic resonance (ODMR)**

I. Introduction

NV centers in diamond are color defects that are stable at room temperature [1]. The electronic level structure of the NV centers is modified in the presence of an external magnetic field (e.g. due to magnetic nanoparticles in vicinity of diamond nanoparticles containing NV centers), thus enabling NV centers to be leveraged for atomic-sized quantum sensors [2]. Various protocols, including optically detected magnetic resonance (ODMR) [3], spin relaxometry using T_1 measurement [4], Ramsey magnetometry, etc., can be used to identify environments with fluctuating magnetic fields. The necessary measurement schemes for interrogating changes in the longitudinal spin relaxation time (T_1) are purely optical, with no requirement of introducing microwave signals [4]. Thus, T_1 relaxometry protocols are naturally favorable for studying tissues, cells, and other biological samples. Nanodiamonds (NDs) containing NV centers are stable and do not suffer from robustness issues such as bleaching and blinking and can be easily incorporated inside living cells [5].

In NDs containing hundreds of NVs, their individual spins can be arbitrarily oriented along any of the four possible directions in the diamond lattice. As a result, the impact of an external magnetic field will be diffused, and not additive on the entire NV population. The other limitation of highly dense NV nanodiamond samples is the screening effect of surrounding NVs on any individual NV. Additionally, NVs, too closely spaced, will screen the impact of external magnetic field on each other, and require large amount of laser power for polarization, that may not be feasible for imaging of cells or biological tissues [6]. These effects limit the sensing performance of NDs containing large density of NVs [7]. In this work, we have explored the feasibility of using NDs with only 4 NVs each (4NV/ND), as an alternative for biosensing.

II. Methods and Results

We have investigated changes in T_1 relaxometry and ODMR of 4NV/NDs due to magnetic stimulus originating from magnetic nanoparticles (MNPs) in their vicinity, through numerical simulations and experiments.

Overview of simulations: T_1 of NVs depends on the transverse component of magnetic field strength $B_{\perp,\mathrm{spins}}$ produced by neighboring spins and the associated dipolar fluctuation rates $R_{\mathrm{dipole,spins}}$ [4], and is denoted by:

$$\Gamma_1 = \frac{1}{T_1} = \Gamma_1^{\mathrm{bulk}} + 3\gamma_e^2 B_{\perp,\mathrm{spins}}^2 \left(\frac{R_{\mathrm{dipole,spins}}}{R_{\mathrm{dipole,spins}}^2 + \omega_0^2} \right) \quad (1)$$

where γ_e is the gyromagnetic ratio, ω_0 is the zero-field splitting, and Γ_1^{bulk} (bulk contribution) depends on the material. We modeled $B_{\perp,\mathrm{spins}}$ and $R_{\mathrm{dipole,spins}}$ specifically for the 4NV/ND system, by extending the model presented by Li et al. [4]. Neighboring MNPs and the surface spin associated with an ensemble of 4NV/NDs were modeled based on dipolar interactions given by equation (1) with suitable material parameters. The number of photons emitted after a specified dark time (relaxation time) τ from an ensemble of NDs is heavily dependent on the thermal relaxation rate [4], and can be modeled as: $N_{photon}(\Gamma_1) = A\left(1 + Be^{-\Gamma_1 \tau}\right)$, where A is a function of the protocol used, and B is a parameter dependent on the single NV photon emission process. Detailed analysis of the simulated results (to be included in full proceedings) yields the number of molecules that could be detected by such a sensor, and the effect of noise and environmental parameters on the sensitivity. The simulated photon distributions and T_1 were experimentally verified, as described below.

Overview of experimental platform: Fig. 1(a) shows a schematic of the experimental setup and 4NV/ND samples. We have used carboxylated fluorescent 4NV/NDs (Sigma Alrich) with average diameter of $35\,\mathrm{nm}$. Iron oxide MNPs with $5\,\mathrm{nm}$ average size were used for studying sensitivity of the platform. Iron oxide MNPs are biocompatible and possess remarkable paramagnetic properties. The ND stock sample $(1\,\mathrm{mg\,mL^{-1}})$ was diluted and sonicated to break apart large clusters, and dropcasted on a cover slip. No additional pre-processing was performed, as the primary goal of the experiments was to observe the ensemble performance of the spin systems. For T_1 and ODMR measurements on NDs, we used a home-built confocal microscope (Fig. 1(b)). After imaging the sample with adequate resolution, regions with high enough parti-

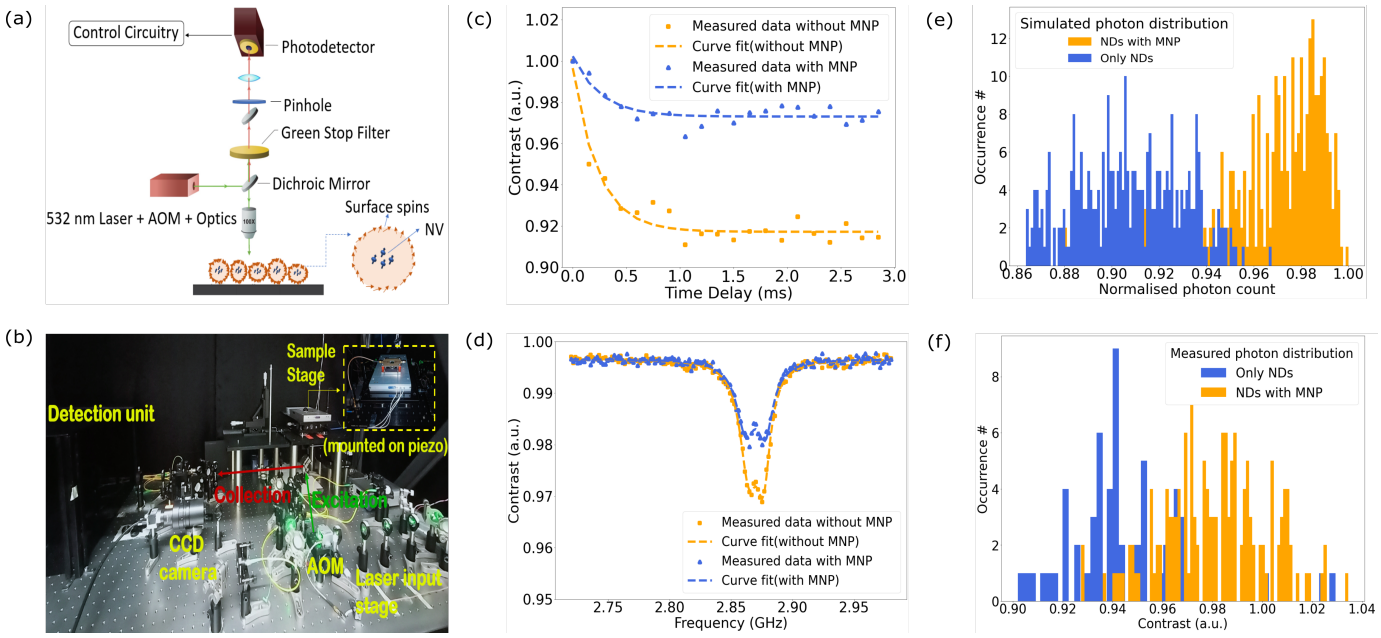

Fig. 1. (a) Simplified schematic of the experimental setup. The inset shows nano-diamond with the distribution of NV spins (blue) and surface spins (red). (b) Image of the fiber-based, confocal setup. The primary components in the setup are marked in the figure (Acousto-optic modulator (AOM), sample stage on piezo, detection unit, CCD camera). The green and red arrows denote the excitation and emission paths, respectively. (c) Contrast vs time delay plots with and without MNPs. Exponential fitting of these plots gives $T_1 = 238 \pm 23\,\mu s$ and $T_1 = 26 \pm 8\,\mu s$ for only NDs and NDs with MNPs respectively. (d) Optically detected magnetic resonance of NDs with and without MNPs. (e) Simulated photon distribution of NDs with and without MNPs. (f) Experimental data of photon distribution with and without MNPs.

cle counts were selected for performing the measurements. MNPs were dropcasted on the sample with a micropipette. Fluorescence imaging of the NDs offers an approximate idea about the number of NV centers or NDs available in the ensemble. To measure the T_1 of NV centers, the NVs were polarized by a laser pulse of $100\,\mu s$ duration followed by a laser readout pulse of $1\,\mu s$ applied after delay $= \tau$ ranging from $20\,ns$ to $3\,ms$. Continuous wave measurement protocols were used for recording ODMR. Measurements were repeated with appropriate averaging for adequate signal-to-noise ratio.

III. Discussion/ Interpretation

A suitable location of the sample was chosen for imaging, by scanning the sample within the range of the piezo stage ($200\,\mu m \times 200\,\mu m \times 200\,\mu m$), and identifying a diffraction-limited spot ($250\,nm$) with identical photon counts as used in the simulations. We ensured that the same spot was used for recording data with and without MNPs. We observed a decrease in T_1 (from $238\,\mu s$ to $26\,\mu s$) after adding $2\,\mu L$ of $5\,mg\,mL^{-1}$ MNPs on to the cover slip containing 4NV/NDs (Fig. 1(c)). ODMR measurement also showed notable reduction in contrast after adding the MNPs (Fig 1(d)). The T_1 shift is easily resolved from the standard deviation associated with multiple measurements on the sample. Fig. 1(e) shows simulation results of the ND ensemble with and without the MNPs, which shows the same trend as experimentally measured data (Fig 1(f)). We have plotted the contrast of the detected photons instead of photon distribution in the experimental data, as the former is not impacted by laser fluctuations. As contrast and photon statistics are fundamentally the same, this causes no loss of information. Our protocol utilized pulse widths of $100\,\mu s$ for polarization pulse and $1\,\mu s$ for detection pulse, whereas in NDs with high NV concentration ($3\,ppm$), it takes around $1\,ms$ to polarize the NVs [3]. Therefore, the entire measurement scheme takes less than ten minutes to execute instead of several minutes to few hours required for high NV-density ND samples. On the other hand, single NVs typically require $1\,\mu s$ of polarization time but suffer from low photon counts, and hence lower sensitivity. Our results suggest that using NDs with few NVs offers a good compromise.

IV. Conclusion

We have demonstrated the feasibility of using ensemble of NDs, each containing few NVs, for high resolution sensing of magnetic nanoparticles. This scheme can be extended to biosensing of a wide variety of magnetically tagged biomolecules with ultra-low concentrations. Adding microwave stimulus in the form of π-pulses can make the protocol more robust against noise [8] and will be explored in future work.

Acknowledgments

A.M. and M.P. acknowledge the Prime Minister's Research Fellows (PMRF) Scheme for supporting their Ph.D. fellowships. This work was partially supported through a grant from Department of Science and Technology (DST), Government of India [grant No. DST/ICPS/QuST/Theme-2/2019/Q-58].

REFERENCES

[1] R. Schirhagl, K. Chang, M. Loretz, and C. L. Degen, "Nitrogen-vacancy centers in diamond: nanoscale sensors for physics and biology," *Annual Review of Physical Chemistry*, vol. 65, no. 1, pp. 83–105, 2014.

[2] R. D. Allert, K. D. Briegel, and D. B. Bucher, "Advances in nano- and microscale NMR spectroscopy using diamond quantum sensors," *Chemical Communications*, vol. 58, no. 59, pp. 8165–8181, 2022.

[3] F. Gorrini, R. Giri, C. E. Avalos, S. Tambalo, S. Mannucci, L. Basso, N. Bazzanella, C. Dorigoni, M. Cazzanelli, P. Marzola, A. Miotello, and A. Bifone, "Fast and Sensitive Detection of Paramagnetic Species Using Coupled Charge and Spin Dynamics in Strongly Fluorescent Nanodiamonds," *ACS Applied Materials & Interfaces*, vol. 11, no. 27, pp. 24 412–24 422, 2019.

[4] C. Li, R. Soleyman, M. Kohandel, and P. Cappellaro, "SARS-CoV-2 Quantum Sensor Based on Nitrogen-Vacancy Centers in Diamond," *Nano Letters*, vol. 22, no. 1, pp. 43–49, Jan 2022.

[5] M. Barzegar Amiri Olia, P. S. Donnelly, L. C. Hollenberg, P. Mulvaney, and D. A. Simpson, *ACS Applied Nano Materials*, vol. 4, no. 10, pp. 9985–10 005, 2021.

[6] A. H. Marblestone, B. M. Zamft, Y. G. Maguire, M. G. Shapiro, T. R. Cybulski, J. I. Glaser, D. Amodei, P. B. Stranges, R. Kalhor, D. A. Dalrymple, D. Seo, E. Alon, M. M. Maharbiz, C. J. M, R. J. M, B. E. S, C. G. M, and K. K. P, "Physical principles for scalable neural recording," *Frontiers in computational neuroscience*, vol. 7, p. 137, 2013.

[7] F. Perona Martínez, A. C. Nusantara, M. Chipaux, S. K. Padamati, and R. Schirhagl, "Nanodiamond relaxometry-based detection of free-radical species when produced in chemical reactions in biologically relevant conditions," *ACS Sensors*, vol. 5, no. 12, pp. 3862–3869, Dec 2020.

[8] M. Mrózek, D. Rudnicki, P. Kehayias, A. Jarmola, D. Budker, and W. Gawlik, "Longitudinal spin relaxation in nitrogen-vacancy ensembles in diamond," *EPJ Quantum Technology*, vol. 2, pp. 1–11, 2015.